Investigations of Ion Channel Structure-Function Relationships Using Molecular Modeling and Experimental Biochemistry

Thesis by

Donald Eugene Elmore, Jr.

In Partial Fulfillment of the

Requirements for the Degree of

Doctor of Philosophy

California Institute of Technology

Pasadena, California

2004

(Defended April 22, 2004)

Chapter 7: Computational Determination of Nicotine Conformations in the Gas Phase and in Aqueous Solution

Background

Nicotine (Fig. 7.1) is a major drug of abuse that acts as a potent agonist of the nicotinic acetylcholine receptor (nAChR). Related nicotinic species have been proposed as treatments for conditions ranging from cognitive and attention deficits to Parkinson's disease to smoking cessation (Bannon et al., 1998; Eglen et al., 1999; Holladay et al., 1997). A thorough understanding of the geometric and electronic structure of nicotine would aid efforts to elucidate receptor structure-function relationships and design new pharmaceuticals. Several early experimental and theoretical studies investigated the relative stabilities of different nicotine conformers (Barlow et al., 1986; Berthelot et al., 1991; Chynoweth et al., 1973; Cox et al., 1986; Hacksell and Mellin, 1989; Kier, 1968; Koo and Kim, 1965; Pitner et al., 1978; Pullman et al., 1971; Radna et al., 1973; Seeman, 1984; Whidby et al., 1979; Whidby and Seeman, 1976). Much of this work focused on three conformational aspects of nicotine: the position of the N8-methyl substituent relative to the pyridine ring (*cis* or *trans*); the relative orientation of the two rings; and the conformation of the pyrrolidine ring. Crystal structures of both the monoprotonated and diprotonated forms of nicotine as iodide salts show the two rings nearly perpendicular to one another and a *trans* N8 group (Barlow et al., 1986; Koo and Kim, 1965). However, these crystal structures do not give direct insight into relative conformer populations present in solution. Moreover, these crystals were grown from ethanol, in which nicotine might adopt a different conformation than in water. NMR studies have probed nicotine solution phase conformations (Chynoweth et al., 1973; Cox et al., 1986; Pitner et al., 1978; Seeman, 1984; Whidby et al., 1979; Whidby and Seeman, 1976). Early NOE work proposed a *cis* N8-methyl group (Chynoweth et al., 1973), but Whidby and Seeman

refuted this conclusion estimating an approximately 10:1 *trans*/*cis* equilibrium ratio for nicotine (Whidby and Seeman, 1976). This latter study was conducted at very low pH to suppress N8-inversion and therefore involved direct characterization of the diprotonated form, making conclusions about the physiologically relevant monoprotonated species necessarily indirect. Further NMR structural studies proposed that the pyridine and pyrrolidine rings are approximately perpendicular to one another and that the pyrrolidine ring adopts an envelope conformation with N8 out of plane (Pitner et al., 1978). However, these NMR studies were performed in a $CDCl_3/CFCl_3$ solvent mixture, which could lead to different conformational stabilities than aqueous solvent.

Figure 7.1: Nicotine protonation states and numbering of nicotine used in this chapter.

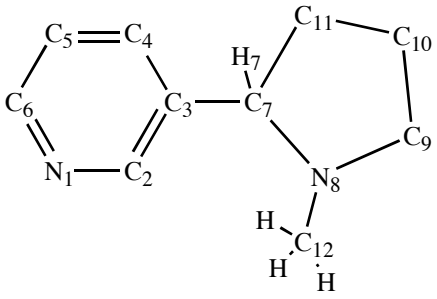

neutral (**0**)

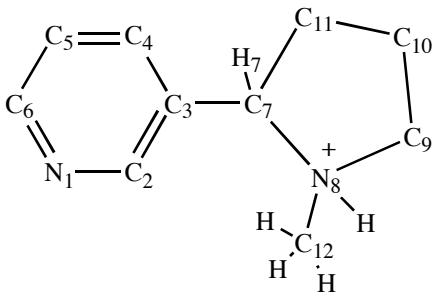

singly protonated (**+**)

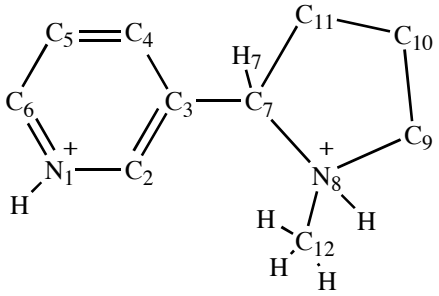

doubly protonated (**++**)

Previous computational studies of nicotine conformation employed PCILO (Pullman et al., 1971), molecular mechanics (Hacksell and Mellin, 1989), INDO (Radna et al., 1973; Seeman, 1984), AM1 (Berthelot et al., 1991), and extended Hückel (Kier, 1968) methods. These studies generally produced low energy conformers similar to those found experimentally, with the N8-methyl group *trans* and the two rings approximately perpendicular to one another. All of these calculations involved levels of theory well below the current state of the art and were conducted in the gas phase, ignoring possible effects arising from interactions with water. Recently, more modern computational techniques have been used to study the conformations of other nAChR ligands: ACh (Edvardsen and Dahl, 1991; Margheritis and Corongiu, 1988; Segall et al., 1998), epibatidene (Campillo et al., 1998), and anatoxin-a (Thompson et al., 1992), and it seemed appropriate to perform a contemporary study on nicotine. This was done by using a combination of quantum mechanical gas-phase methods and two very different solvation models. One model used explicit TIP4P (Jorgensen et al., 1983) water with the OPLS force field (Jorgensen et al., 1996) developed and applied by Jorgensen along with Monte Carlo (MC) statistical perturbation theory (SPT) methods (Jorgensen, 1989). SPT/OPLS methods have been used to calculate solvent effects for a variety of chemical systems, including heterocycles similar to nicotine, such as histamine, imidazone, and nicotinic and isonicotinic acids (Nagy and Durant, 1996; Nagy et al., 1994; Nagy et al., 1993; Nagy and Takács-Novák, 1997). The second solvation model applied is a recently developed quantum mechanical continuum method, SM5.42R (Li et al., 1998; Zhu et al., 1998), which has been parameterized for a number of HF and DFT methods. It has

produced good results for a wide range of solutes, including N-containing species which are sometimes problematic for solvation methods.

Energetic Profile for Relative Pyridine/Pyrrolidine Ring Rotations

Rotation around the C3-C7 bond was investigated using molecular mechanics (MMFF94) and semiempirical (AM1) methods implemented in SPARTAN 5.0. This was done for all nicotine protonation states (Fig. 7.1), which will be referred to as **0** (unprotonated), **+** (singly protonated), **++** (doubly protonated). The rotational profiles were performed by freezing the H7-C7-C1-C2 dihedral angle at approximately 5° intervals and optimizing the remainder of the structure. All profiles were generally like the **+** MMFF94 profiles shown in Fig. 7.2 with two minima. These rotamers, labeled **A** and **B**, have dihedral angles close to 0° and 180°, respectively, which place the pyridine and pyrrolidine rings roughly perpendicular to one another as seen in previous work (Hacksell and Mellin, 1989; Kier, 1968; Pitner et al., 1978; Pullman et al., 1971). Rotational barriers between **A** and **B** are consistently higher for the *cis* species (6-8 kcal/mol versus about 3 kcal/mol for *trans*), which is consistent with increased steric interactions between the N8-methyl group and the pyridine ring in that species. Nonetheless, these barriers are low enough to generally allow rapid rotation between the **A** and **B** species.

Figure 7.2: MMFF94 rotational profile for singly protonated (+) nicotine species**.**

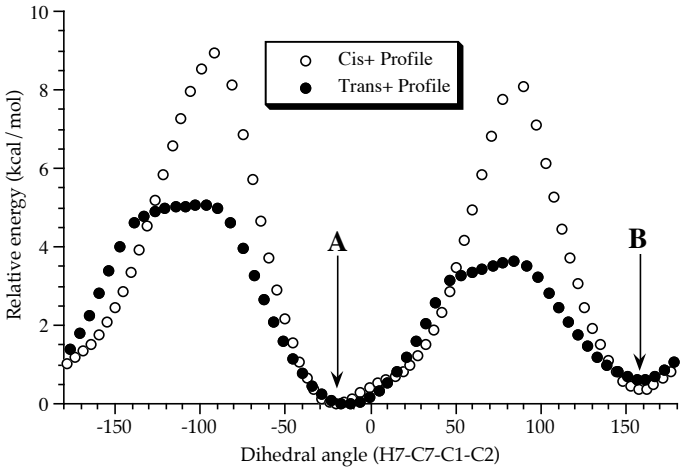

Gas-Phase Structures and Energetics

Gas-phase optimized structures were therefore calculated for the **A** and **B** rotamers of each protonation state at the HF/6-31G** level; HF/6-31G** frequency calcualtions were used to verify these were true minima. All *ab initio* calculations were performed with the Gaussian 94 suite (Frisch et al., 1995). Although the major contributors in aqueous solution may not all be gas-phase minima (Colominas et al., 1999), this seems unlikely in the present system that has relatively few degrees of conformational freedom. Pictures of the optimized **+** species can be seen in Fig. 7.3, and selected geometrical quantities for all structures are given in Table 7.1. The rings remain relatively perpindicular in these optimizations. The intramolecular N3-N8 distances are longer for **A** rotamers; this trend is more pronounced in *trans* than *cis* species. These differences might be related to differences in solvation discussed below. As well, the N-N distance increases between **+** and **++** species, as observed in crystal structures (Barlow

et al., 1986; Koo and Kim, 1965), apparently as two positively charged centers repel each other.

Table 7.1: Selected geometric attributes of nicotine species optimized at HF/6-31G**.[a]

Species	N1-N8	H7-C7-C3-C2	C7-N8-C9-C10	N8-C9-C10-C11	C9-C10-C11-C7
***cis*+ A**	4.582	-19.0	37.3	-18.5	-6.7
***cis*+ B**	4.529	159.8	37.4	-18.8	-6.2
***trans*+A**	4.655	-5.9	-25.7	1.3	23.3
***trans*+ B**	4.385	178.0	-27.7	4.0	21.0
***cis* A**	4.633	-18.9	36.8	-16.9	-6.9
***cis* B**	4.537	160.6	37.2	-17.4	-6.4
***trans* A**	4.793	16.5	-42.3	25.7	-1.4
***trans* B**	4.247	-164.7	-42.3	25.6	-1.2
***cis*++ A**	4.749	-5.6	26.4	-41.0	40.5
***cis*++ B**	4.708	140.7	-4.4	-22.3	40.5
***trans*++ A**	4.737	1.7	-30.7	7.6	17.8
***trans*++ B**	4.546	162.6	-24.0	-1.5	26.0

[a]Distances are in Å and angles are in degrees; pyrrolidine dihedral angles are given to the right of the bold line.

Pyrrolidine ring conformation was ambiguous in previous work. NMR studies on nicotine and closely related compounds have implied that the ring has an envelope conformation with the N8 atom out of plane in nonaqueous solution where the **0** species would have been present (Pitner et al., 1978; Seeman, 1984; Whidby et al., 1979). Conversely, the **+** and **++** crystal structures show species with more twisted conformations (Barlow et al., 1986; Koo and Kim, 1965). To address this, several ring conformations were explored with AM1 and HF/6-31G** calculations, leading to the most stable conformers shown in Fig. 7.3 and Table 7.2. The *trans***0** pyrrolidine has an envelope conformation analogous to NMR results. However, the *trans***+** and *trans***++** species alter their envelope conformation to place the C7 atom out of plane, which is

different than in crystal structures (Barlow et al., 1986; Koo and Kim, 1965). All *cis***0** and *cis***+** structures have similar envelope conformations, with the N8-atom out of plane, although the rest of the ring is less planar than in *trans***0** conformers. Doubly protonated *cis***++ A** and **B** structures show different conformations than other protonation states, with C10 and C11 out of plane, respectively.

Figure 7.3: HF/6-31G** optimized structures of singly protonated nicotine species. Key: Black: carbon, Grey: nitrogen, White: hydrogen.

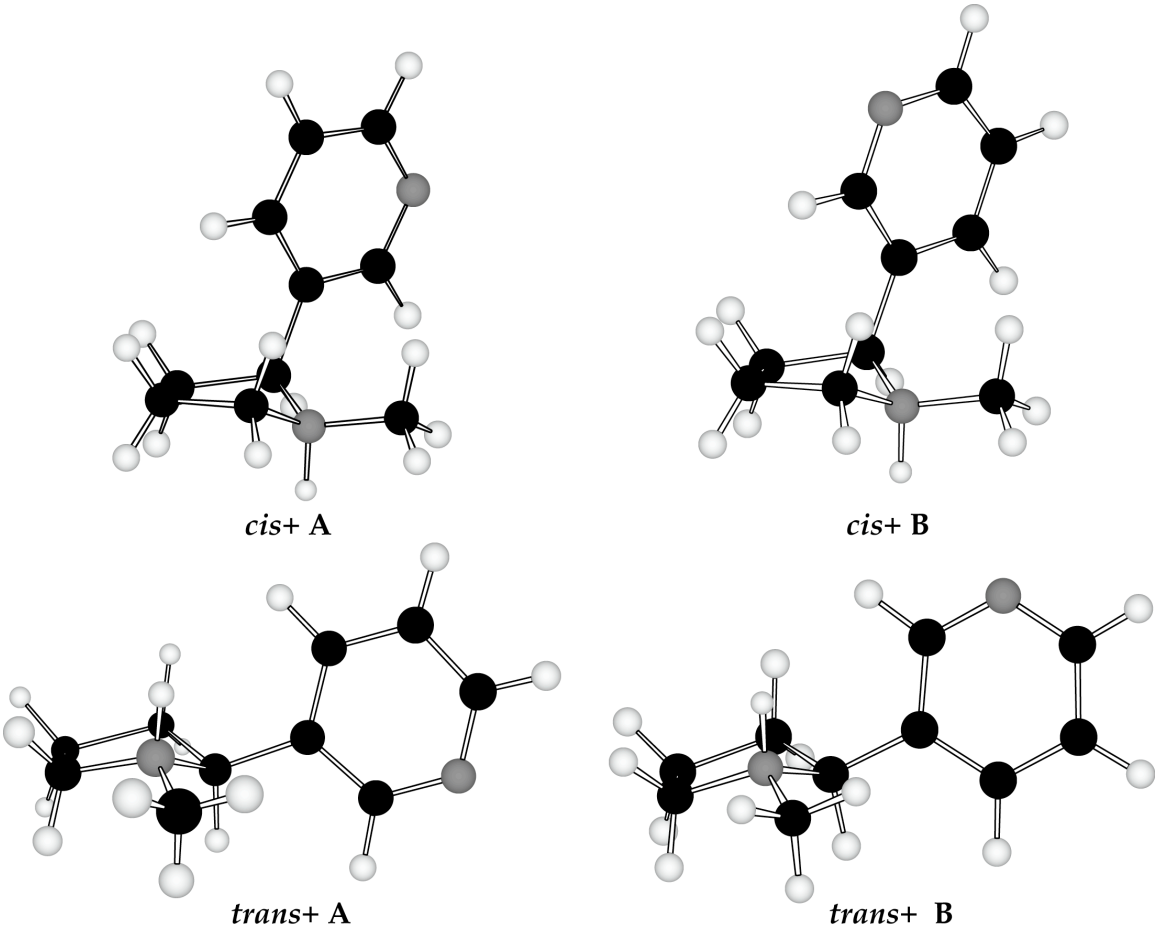

Energetic comparisons of the conformers were done using MP2/6-31G** and B3LYP/6-31G** single point calculations on the optimized HF/6-31G** structures.

These energies were combined with thermal energy (TE) and entropy (S) estimates from the HF/6-31G** frequency calculations to obtain ΔG values by the following relationship: $\Delta G = \Delta E + \Delta TE - 298(\Delta S)$. Relevant quantities from these calculations are given in Table 7.2. For all protonation states at all computational levels, *trans* species are prediced to be more stable than *cis*, consistent with steric considerations. Little difference is seen between **A** and **B** rotamers of most species. However, the **A/B** difference is larger for the **0** and **++** *trans* stereoisomers. The ΔG values predict a larger energy gap between *cis* and *trans* steroisomers than ΔE values because the *trans* species are more entropically favorable than the more compact and restricted *cis*; this effect is largest for the **+** species.

Table 7.2: Relative gas-phase ΔG values and thermal energy and entropy corrections for all nicotine species considered[a]

Species/ Conformer	HF/6-31G** ΔG	MP2/6-31G** //HF/6-31G** ΔG	B3LYP/6-31G** //HF/6-31G** ΔG	ΔTE + 298x(ΔS) relative to *trans*A
***cis*+ A**	4.32	2.87	4.09	1.19
***cis*+ B**	4.38	2.94	4.15	1.24
***trans*+A**	0.00	0.00	0.06	0.00
***trans*+ B**	0.00	0.01	0.00	-0.03
***cis* A**	5.21	4.30	4.83	0.67
***cis* B**	5.44	4.53	5.08	0.73
***trans* A**	0.00	0.00	0.00	0.00
***trans* B**	0.48	0.52	0.44	-0.04
***cis*++ A**	3.41	2.51	2.69	0.23
***cis*++ B**	3.60	2.75	3.18	0.18
***trans*++ A**	0.00	0.00	0.00	0.00
***trans*++ B**	1.03	1.07	1.03	0.07

[a] All values are given in kcal/mol.

Inclusion of Solvation in Energetic Calculations

Explicit solvation calculations on the **+** conformers were performed using BOSS version 3.8 (Jorgensen, 1997). For these, the optimized HF/6-31G** geometries were used for solute structures. Calculations used an approximately 25 Å cubic cell of 500 TIP4P (Jorgensen et al., 1983) water molecules and the isothermic-isobaric ensemble (NPT) at 25 °C and 1 atm. Standard OPLS all-atom Lennard-Jones parameters (Jorgensen et al., 1996) and CHELPG charges (Breneman and Wiberg, 1990) fit to the HF/6-31G** wavefunction were used for the solutes, as previously recommended (Carlson et al., 1993). Solvent-solvent and solute-solvent interactions were cut off at 12 and 10 Å, respectively, with potential functions quadradically feathered to zero over the final 0.5 Å. Perturbations were performed with ten steps of double-wide sampling to give 20 simulation windows; for each window 2×10^6 and 4×10^6 conformations were sampled for equilibrium and averaging phases, respectively. Volume and solute moves were attempted every 1000 and 50 configurations, respectively, and ranges for moves were set to allow approximately 40% of the moves to be accepted. A thermodynamic cycle of $\Delta\Delta G_{sol}$ values from the perturbations performed are given in Fig. 7.4. These $\Delta\Delta G_{sol}$ values from the SPT/OPLS method can then be combined with the calculated gas-phase values (Table 8.2) to determine relative ΔG values for each of the **+** species in water (Table 8.3).

The HF/6-31G*, HF/cc-pVDZ, and BPW91/6-31G* parameterizations of the SM5.42R method were also used to determine ΔG_{sol} for **+** species. Again, HF/6-31G** structures were used as rigid solutes. The $\Delta\Delta G_{sol}$ values for these calculations are given in Table 7.4; overall relative ΔG values for conformers using these solvation energies

along with TE and S estimates from HF/6-31G** gas-phase frequency calculations are in Table 7.5. As can be seen, SM5.42R $\Delta\Delta G_{sol}$ values are not identical in magnitude to those predicted using the SPT/OPLS method; most striking is the *trans*+**B**/*cis*+**A** difference. Nonetheless, both methods predict the same qualitative order of ΔG_{sol} values for these conformers.

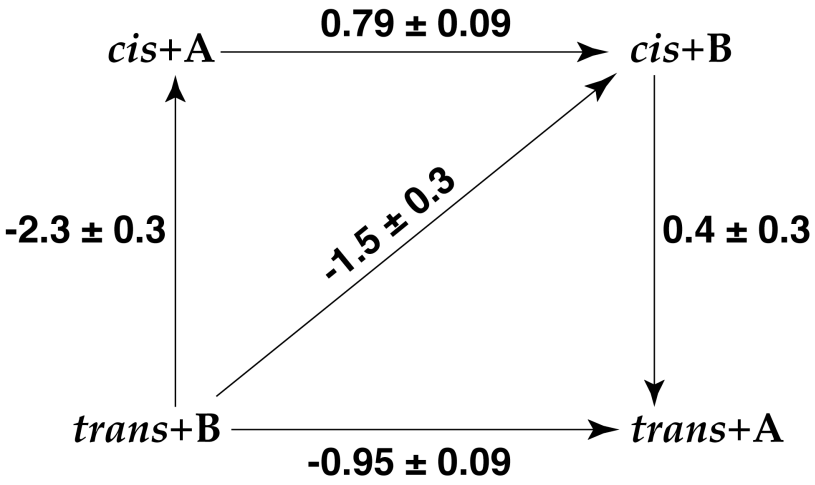

Figure 7.4: Thermodynamic cycle of $\Delta\Delta G_{sol}$ values for singly protonated nicotine species calculated with SPT/OPLS. All values are in kcal/mol.

Table 7.3: Relative ΔG of singly protonated species including computed solvation effects from SPT/OPLS; Predicted relative equilibrium percentages at 25 °C in parentheses[a]

Species/ Conformer	HF/6-31G**	MP2/6-31G**// HF/6-31G**	B3LYP/6-31G**// HF/6-31G**
***cis*+ A**	3.1 ± 0.3 (0.4)	1.6 ± 0.3 (5.3)	2.8 ± 0.3 (0.8)
***cis*+ B**	4.0 ± 0.3 (0.1)	2.5 ± 0.3 (1.1)	3.7 ± 0.3 (0.2)
***trans*+A**	0.0 (82.8)	0.0 (78.1)	0.0 (80.0)
***trans*+ B**	0.95 ± 0.09 (16.7)	0.96 ± 0.09 (15.5)	0.89 ± 0.09 (18.9)

[a] ΔG values are given in kcal/mol.

The overall ΔG values for the species lead directly to predicted equilibrium ratios of each species in solution using a Boltzmann distribution, given for 25 °C in Tables 7.3 and 7.5. Despite quantitative differences, all methods clearly predict that no more than 6% of the species should be in a *cis* conformation, implying the experimental 1:10 *cis*/*trans* ratio may be an upper limit of *cis* present (Whidby and Seeman, 1976). As well, in the receptor binding site, which is not purely aqueous, one would expect the relative proportion of *cis* to be lower than in bulk water since *cis* is stabilized relative to *trans* by aqueous solvation. These percentages do emphasize one difference between the solvation methods, as SPT/OPLS predicts mainly *trans***+A** would be present while SM5.42R predicts that the amounts of *trans***+A** and **B** would be more nearly equal.

Table 7.4: Relative $\Delta\Delta G_{sol}$ values of singly protonated species calculated with SM5.42R at various levels of theory[a]

Species/Conformer	HF/6-31G*// HF/6-31G**	HF/cc-pVDZ// HF/6-31G**	BPW91/6-31G*// HF/6-31G**
***cis*+ A**	0.000	0.000	0.000
***cis*+ B**	0.089	0.640	0.043
***trans*+A**	0.658	1.223	0.632
***trans*+ B**	0.889	1.382	0.817

[a] ΔG values are given in kcal/mol.

Table 7.5: Relative ΔG of singly protonated species including computed solvation effects from SM5.42R; Predicted relative equilibrium percentages at 25 °C in parentheses[a]

Species/Conformer	HF/6-31G*// HF/6-31G**	HF/cc-pVDZ// HF/6-31G**	BPW91/6-31G*// HF/6-31G**
***cis*+ A**	3.68 (0.1)	3.28 (0.2)	3.44 (0.2)
***cis*+ B**	3.81 (0.1)	4.01 (0.1)	3.58 (0.1)
***trans*+A**	0.00 (59.0)	0.00 (58.7)	0.00 (54.6)
***trans*+ B**	0.22 (40.8)	0.21 (41.0)	0.11 (45.1)

[a] ΔG values are given in kcal/mol.

Both solvation methods show two trends in ΔG_{sol} for these species: 1) *cis* species solvate better than *trans* and 2) **A** rotamers solvate better than **B**. The *cis*/*trans* difference can be rationalized by considering solvent accessible surface area (SASA) values calculated by BOSS (Jorgensen, 1997). *Cis* species have lower SASA (381 $Å^2$) than *trans* (398 $Å^2$) and therefore reduce the less favorable interactions that occur at the interface of the hydrophobic portions of the solute and water. Also, *cis* more fully exposes the N^+-H substructure likely to be best solvated. The radial distribution function of water oxygen atoms around the N^+-H proton shows that the first solvation shell has a similar population in *cis* and *trans* species, while a solvation difference arises with a more closely held second shell in *cis*. This difference in second solvation shells could explain why the OPLS/SPT method predicts a larger *cis*/*trans* $\Delta\Delta G_{sol}$ than SM5.42R. **A** rotamers possibly are better solvated than **B** because they have a larger separation between the two oppositely charged regions. Since this change in N-N distance is slightly larger between the *trans*+ than the *cis***+** rotamers, it is reasonable that the relative stabilization of the **A** rotamer is slightly larger in the *trans***+** species for almost all models.

Calculation of ΔG_{sol} of the other nicotine protonation states (**0** and **++**) was performed using the SM5.42R HF/6-31G* parameterized model on HF/6-31G** geometries. This model was applied to these systems in lieu of SPT/OPLS simulations because it produced similar qualitative trends for the singly protonated species at a fraction of the computational expense. The same *cis*/*trans* solvation trend seen for **+** species was seen for other protonation states, and *trans* species are still predicted to be most stable in aqueous solution. But, the **B** rotamers for both **0** and **++** species showed

better solvation than the **A** ones. Thus, in species where the N atoms carry a similar charge, solvation appears to improve with decreased N-N distance.

Relevance to Other Work on Nicotinic Receptors and Agonists

These predictions of nicotine conformation can be considered in light of previous studies estimating the geometrical relationship between "pharmacophore" groups important for nicotine binding, such as optimal N-N distances. Earlier work proposed a N-N distance of 4.8 Å (Sheridan et al., 1986), which is quite close to the calculated *trans***+A** N-N distance (4.655 Å). Later work including the high-affinity nAChR ligand epibatidine proposed a longer optimal N-N distance of 5.5 Å (Glennon et al., 1994). Although this estimate is significantly longer than the *trans***+A** N-N distance, the *trans***+A** conformer does have the maximum N-N distance of the structures considered in this work (Table 7.1), which might provide evidence that it represents the active conformation. Additional research on conformationally restricted nicotine analogs, such as those described in recent reviews, may give increased insight into the physiological difference between the rotamers considered (Glennon and Dukat, 1996; Holladay et al., 1997).

Understanding the conformation of nicotine can also be useful for considering some interesting observations made by Dougherty and co-workers about the activation of nAChR by nicotine. Experimental and computational work reported by Zhong et al. clearly showed that the natural agonist acetylcholine interacts strongly with a trytophan residue at the binding site of the nAChR through a cation-π interaction (Zhong et al., 1998). This assertion has been supported by the crystal structure of the acetylcholine

binding protein with a bound positively charged HEPES molecule (Brejc et al., 2001). However, subsequent work has shown that although nicotine activates the receptor it does *not* appear to interact at the binding site through an analogous cation-π interaction (Beene et al., 2002). The computational predictions about nicotine conformation described in this chapter have helped to provide a starting point for current computational and experimental work performed by Petersson and Cashin attempting to explain these unusual observations about the interactions between nicotine and the nAChR (Cashin, Petersson, et al, unpublished work).

References

Bannon, A. W., M. W. Decker, M. W. Holladay, P. Curzon, D. Donnelly-Roberts, P. S. Puttfarcken, R. S. Bitner, A. Diaz, A. H. Dickenson, R. D. Porsolt, M. Williams, and S. P. Arneric. 1998. Broad-spectrum, non-opioid analgesic activity by selective modulation of neuronal nicotinic acetylcholine receptors. *Science* 279:77-81.

Barlow, R. B., J. A. K. Howard, and O. Johnson. 1986. Structures of nicotine monomethyl iodide and nicotine monohydrogen iodide. *Acta. Cryst.* C42:853-856.

Beene, D. L., G. S. Brandt, W. Zhong, N. M. Zacharias, H. A. Lester, and D. A. Dougherty. 2002. Cation-pi interactions in ligand recognition by serotonergic (5-HT3A) and nicotinic acetylcholine receptors: the anomalous binding properties of nicotine. *Biochemistry* 41:10262-9.

Berthelot, M., M. Decouzon, J.-F. Gal, C. Laurence, J.-Y. Le Questel, P.-C. Maria, and J. Tortajada. 1991. Gas-phase basicity and site of protonation of polyfunctional molecules of biological interest: FT-ICR experiments and AM1 calculations on nicotines, nicotinic acid derivatives, and related compounds. *J. Org. Chem.* 56:4490-4494.

Brejc, K., W. J. van Dijk, R. V. Klaassen, M. Schuurmans, J. van Der Oost, A. B. Smit, and T. K. Sixma. 2001. Crystal structure of an ACh-binding protein reveals the ligand-binding domain of nicotinic receptors. *Nature* 411:269-76.

Breneman, C. M., and K. B. Wiberg. 1990. Determining atom-centered monopoles from molecular electrostatic potentials—the need for high sampling density in formamide conformational-analysis. *J. Comput. Chem.* 11:361-373.

Campillo, N., J. A. Páez, I. Alkorta, and P. Goya. 1998. A theoretical study of epibatidine. *J. Chem. Soc., Perkin Trans.* 2:2665-2669.

Carlson, H. A., T. B. Nguyen, M. Orozco, and W. L. Jorgensen. 1993. Accuracy of free energies of hydration for organic molecules from 6-31G*-derived partial charges. *J. Comp. Chem.* 14:1240-1249.

Chynoweth, K. R., B. Ternai, L. S. Simeral, and G. E. Maciel. 1973. Nuclear magnetic resonance studies of the conformation and electron distributions in nicotine and in acetylcholine. *Mol. Pharm.* 9:144-151.

Colominas, C., F. J. Luque, and M. Orozco. 1999. Dimerization of formamide in gas phase and solution. An ab initio MC-MST study. *J. Phys. Chem. A* 103:6200-6208.

Cox, R. H., J. Kao, H. V. Secor, and J. I. Seeman. 1986. Assessment of isolated electronic effects on conformation. NMR analysis of nicotine and related compounds and ab initio studies of model compounds. *J. Mol. Struct.* 140:93-106.

Edvardsen, Ø., and S. G. Dahl. 1991. Molecular structure and dynamics of acetylcholine. *J. Neural Transm.* 83:157-170.

Eglen, R. M., J. C. Hunter, and A. Dray. 1999. Ions in the fire: Recent ion-channel research and approaches to pain therapy. *Trends Pharm. Sci.* 20:337-342.

Frisch, M. J., G. W. Trucks, H. B. Schlegel, P. M. W. Gill, B. G. Johnson, M. A. Robb, J. R. Cheeseman, T. Keith, G. A. Petersson, J. A. Montgomery, K. Raghavachari, M. A. Al-Laham, V. G. Zakrzewski, J. V. Ortiz, J. B. Foresman, J. Cioslowski, B. B. Stefanov, A. Nanayakkara, M. Challacombe, C. Y. Peng, P. Y. Ayala, W. Chen, W. M. Wong, J. L. Andres, E. S. Replogle, R. Gomperts, R. L. Martin, D. J. Fox, J. S. Binkley, D. J. Defrees, J. Baker, J. P. Stewart, M. Head-Gordon, C. Gonzalez, and J. A. Pople. 1995. Gaussian 94. Version 94, D.3. Pittsburgh, PA: Gaussian, Inc.

Glennon, R. A., and M. Dukat. 1996. Nicotine receptor ligands. *Med. Chem. Res.* 6:465-486.

Glennon, R. A., J. L. Herndon, and M. Dukat. 1994. Epibatidine-aided studies toward definition of a nicotine receptor pharmacophore. *Med. Chem. Res.* 4:461-473.

Hacksell, U., and C. Mellin. 1989. Stereoselectivity of nicotinic receptors. *Prog. Brain Res.* 79:95-100.

Holladay, M. W., M. J. Dart, and J. K. Lynch. 1997. Neuronal nicotinic acetylcholine receptors as targets for drug discovery. *J. Med. Chem.* 40:4169-4194.

Jorgensen, W. L. 1989. Free-energy calculations—a breakthrough for modeling organic-chemistry in solution. *Acc. Chem. Res.* 221:184-189.

Jorgensen, W. L. 1997. BOSS. Version 3.8. New Haven, CN: Dept. of Chem., Yale University.

Jorgensen, W. L., J. Chandrasekhar, J. D. Madura, R. Impey, and M. L. Klein. 1983. Comparison of simple potential functions for simulating liquid water. *J. Chem. Phys.* 79:926-935.

Jorgensen, W. L., D. S. Maxwell, and J. Tirado-Rives. 1996. Development and testing of the OPLS all-atom force field on conformational energetics and properties of organic liquids. *J. Am. Chem. Soc.* 118:11225-11236.

Kier, L. B. 1968. A molecular orbital calculation of the preferred conformation of nicotine. *Mol. Pharm.* 4:70-76.

Koo, C. H., and H. S. Kim. 1965. The crystal structure of nicotine dihydroiodide. *Daehan Hwahak Hwojee* 9:134-141.

Li, J., G. D. Hawkins, C. J. Cramer, and D. G. Truhlar. 1998. Universal reaction field model based on ab initio Hartree-Fock theory. *Chem. Phys. Lett.* 288:293-298.

Margheritis, C., and G. Corongiu. 1988. Acetylcholine in water: Ab-initio potential and Monte Carlo simulation. *J. Comp. Chem.* 9:1-10.

Nagy, P. I., and G. J. Durant. 1996. Monte Carlo simulations of the counter ion effect on the conformational equilibrium of the N, N'-diphenyl-guanidinium ion in aqueous solution. *J. Chem. Phys.* 104:1452-1643.

Nagy, P. I., G. J. Durant, W. P. Hoss, and D. A. Smith. 1994. Theoretical analyses of the tautomeric and conformational equilibria of histamine and (aR,bS)-a,b dimethylhistamine in the gas phase and aqueous solution. *J. Am. Chem. Soc.* 116:4898-4909.

Nagy, P. I., G. J. Durant, and D. A. Smith. 1993. Theoretical studies on hydration of pyrrole, imidazole, and protonated imidazole in the gas phase and aqueous solution. *J. Am. Chem. Soc.* 115:2912-2922.

Nagy, P. I., and K. Takács-Novák. 1997. Theoretical and experimental studies of the zwitterion <--> neutral form equilibrium of ampholytes in pure solvents and mixtures. *J. Am. Chem. Soc.* 119:4999-5006.

Pitner, T. P., W. B. Edwards, III, R. L. Bassfield, and J. F. Whidby. 1978. The solution conformation of nicotine. A ^{1}H and ^{2}H nuclear magnetic resonance investigation. *J. Am. Chem. Soc.* 100:246-251.

Pullman, B., P. Courrière, and J. L. Coubeils. 1971. Quantum mechanical study of the conformational and electronic properties of acetylcholine and its agonists muscarine and nicotine. *Mol. Pharm.* 7:397-405.

Radna, R. J., D. L. Beveridge, and A. L. Bender. 1973. Structural chemistry of cholinergic neural transmission systems. II. A quantum theoretical study of the molecular electronic structure of muscarine, nicotine, acetyl-a-methylcholine, acetyl-b-methylcholine, acetyl-a,b-dimethylcholine, and further studies on acetylcholine. *J. Am. Chem. Soc.* 95:3831-3842.

Seeman, J. I. 1984. Recent studies in nicotine chemistry. Conformational analysis, chemical reactivity studies, and theoretical modeling. *Heterocycles* 22:165-193.

Segall, M. D., M. C. Payne, and R. N. Boyes. 1998. An ab initio study of the conformational energy map of acetylcholine. *Mol. Phys.* 93:365-370.

Sheridan, R. P., R. Nilakantan, J. S. Dixon, and R. Venkataraghavan. 1986. The ensemble approach to distance geometry: Application to the nicotinic pharmacophore. *J. Med. Chem.* 29:899-906.

SPARTAN. Version 5.0. Irvine, CA: Wavefunction, Inc.

Thompson, P. E., D. T. Manallack, F. E. Blaney, and T. Gallagher. 1992. Conformational studies on (+)-anatoxin-a and derivatives. *J. Comp. Aided Mol. Design* 6:287-298.

Whidby, J. F., W. B. Edwards, III, and T. P. Pitner. 1979. Isomeric nicotines. Their solution conformation and proton, deuterium, carbon-13, and nitrogen-15 nuclear magnetic resonance. *J. Org. Chem.* 44:794-798.

Whidby, J. F., and J. I. Seeman. 1976. The configuration of nicotine. A nuclear magnetic resonance study. *J. Org. Chem.* 41:1585-1590.

Zhong, W., J. P. Gallivan, Y. Zhang, L. Li, H. A. Lester, and D. A. Dougherty. 1998. From ab initio quantum mechanics to molecular neurobiology: a cation-pi binding site in the nicotinic receptor. *Proc. Natl. Acad. Sci. USA* 95:12088-93.

Zhu, T., J. B. Li, G. D. Hawkins, C. J. Cramer, and D. G. Truhlar. 1998. *J. Chem. Phys.* 109:9117-9133.